EPJ Web of Conferences **120**, 04001 (2016) DOI: 10.1051/epjconf/201612004001
ISMD 2015

Searches for Dark Matter at the ATLAS experiment

Henso Abreu[1] on behalf of the ATLAS Collaboration[a]

[1] *Technion – Israel Institute of Technology. Haifa, 3200003, Israel*

Abstract. Searches for strongly produced dark matters in events with jets, photons, heavy-flavor quarks or massive gauge bosons recoiling against large missing transverse momentum in ATLAS are presented. These "$E_{\mathrm{T}}^{\mathrm{miss}}$+X" signatures provide powerful probes to dark matter production at the LHC, allowing us to interpret results in terms of effective field theory and/or simplified models with pair production of Weakly Interacting Massive Particles. Recent ATLAS results on dark matter searches at LHC Run 1 and the connection to astroparticle physics are discussed.

1 Introduction

Dark Matter existence in the Universe is well established through numerous astrophysical and cosmological observations, as documented in Refs. [1–4], however little is known of its particle nature or its non-gravitational interactions. At the Large Hadron Colliders, one can search for a weakly interacting massive particle (WIMP), denoted by χ, and for interactions between χ and Standard Model particles, see Ref. [5]. Searches conducted at the Large Hadron Collider are especially sensitive at low Dark Matter masses ($m_\chi \leq 10$ GeV), and therefore provide results complementary to direct Dark Matter searches Refs. [6–9] .

Interaction of particles mediating between Dark Matter and Standard Model particles can be described by contact operators in the framework of an effective field theory (EFT) Refs. [10–12] in cases where they are too heavy to be produced directly in the experiment. In the absence of signal, limits can be placed in terms of the effective mass scale of the interaction, M_* and of the $\chi-$nucleon cross-section, $\sigma_{\chi-N}$, as a function of m_χ. In addition to the investigation with the EFT operators, pair production of WIMPs is also investigated within so-called simplified models, where a pair of WIMPs couples to a pair of Standard Models particles explicitly via a new mediator particle, e.g a new vector boson Z'. In this case, limits on M_* and/or m_χ are placed as a function of the mediator mass M_{med}.

A number of dedicated approaches to finding evidence for Dark Matter have been carried out with the ATLAS detector experiment Ref. [13] during Run 1, using typically 20.3 fb^{-1} of data collected at a centre-of-mass energy of $\sqrt{s} = 8$ TeV. So-called mono-X searches take advantage of a variety of different *tag* objects, X, together with large absolute values of missing transverse momentum, $E_{\mathrm{T}}^{\mathrm{miss}}$, in the final state to constitute a clean and distinctive signature. Heavy-quark searches use events with large $E_{\mathrm{T}}^{\mathrm{miss}}$ in association with high-momentum jets of which one or more are identified as jets containing b or top–quarks.

[a] e-mail: habreu@cern.ch

© The Authors, published by EDP Sciences. This is an open access article distributed under the terms of the Creative Commons Attribution License 4.0 (http://creativecommons.org/licenses/by/4.0/).

2 Mono-X Seaches

Tagging events using a variety of recoil objects, mostly stemming from initial state radiation (ISR), gives access to a broad range of EFT operators, as the respective sensitivity depends on the *tag* object in question. All cases require large amounts of $E_{\mathrm{T}}^{\mathrm{miss}}$, coming from the Dark Matter particle, and *tag* objects include single jets or photons as well as electroweak bosons Z and W .

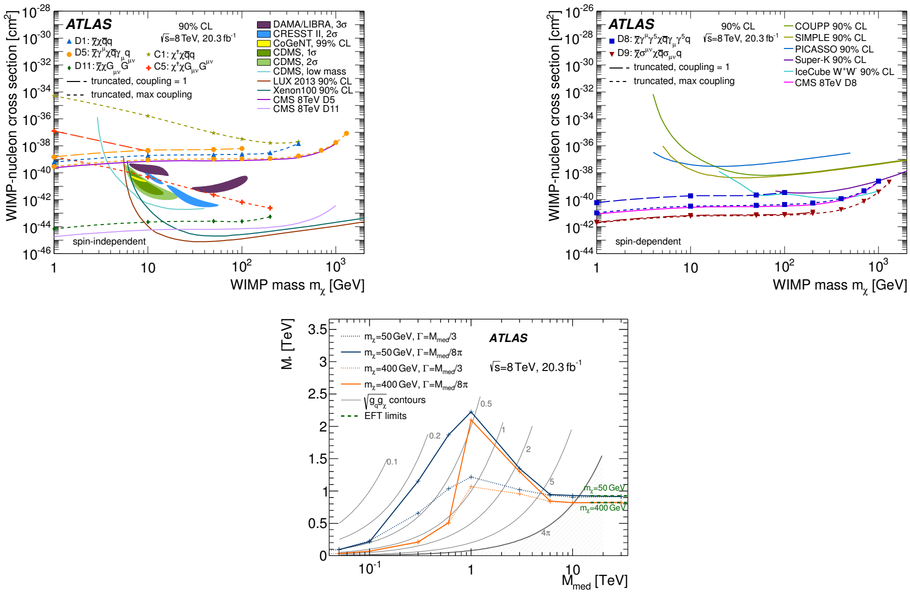

Figure 1. 90% CL limits on spin-independent (top-left) and spin-dependent (top-right) $\sigma_{\chi-N}$ as a function of m_χ for different EFT operators. Observed 95% CL limits on M_* as a function of M_{med} (bottom), assuming a Z'-like bosons in a simplified model and a Dark Matter mass of 50 GeV ad 400 GeV. The width of the mediator is varied between $M_{med}/3$ and $M_{med}/8\pi$. The corresponding limits from EFT models are shown as dashed lines; contour lines indicating a range of values of the product of the coupling constants ($\sqrt{g_q g_\chi}$) are also shown. For details see Refs. [6, 9, 14–30]. Plots taken from Ref. [14]

2.1 Mono-jet+ $E_{\mathrm{T}}^{\mathrm{miss}}$

As introduced in Ref. [14], using a single jet as recoil object gives sensitivity to six EFT operators (D1, D5, D8, D9, D11 and D5). To enhance the expected signal, events are required to contain at least one central jet with transverse momentum p_{T}, larger than both 120 GeV and half of $E_{\mathrm{T}}^{\mathrm{miss}}$. To ensure that the jet is in fact recoiling against the Dark Matter particles, the angle between the jet and the missing transverse momentum in the events is required to be above one. To further suppress background, which is mainly comprised of $Z(\nu\nu)$+jets and $W(\ell\nu)$+jets events, events containing leptons or high-p_{T} isolated tracks are vetoed. As all measurements are consistent with Standard Model expectations, the most sensitive out of nine signal regions, defined by requirements on $E_{\mathrm{T}}^{\mathrm{miss}}$ ranging from 150 GeV to 700 GeV, is used to place limits on $\sigma_{\chi-N}$ for each of the operators under investigation. As an example result of this analysis, inferred 90% confidence level (CL) limits on $\sigma_{\chi-N}$ as a function of m_χ for the spin-independent as well as spin-dependent case for different operators are shown in Fig. 1 (top-left and top-right). To ensure the validity of the EFT approach, the results are also shown after applying a *truncation* procedure as described in Ref. [14]. Limits on M_* as a function of M_{med} in the context of a simplified model are shown in Fig. 1 (bottom).

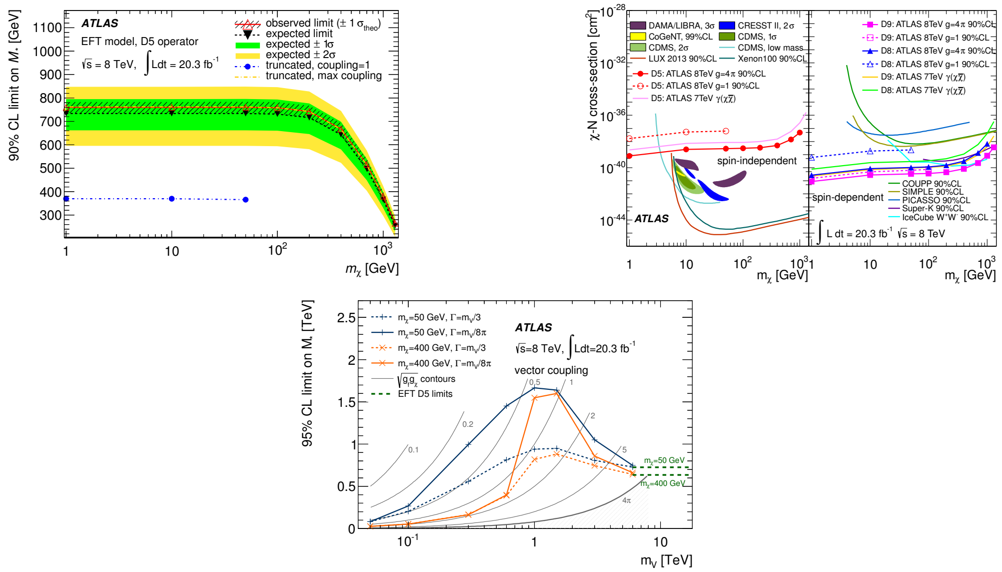

Figure 2. Limits at 90% CL on M_* as a function of m_χ (top-left), for the vector operator D5 . Results where EFT truncation is applied are also shown, assuming coupling values $\sqrt{g_f g_\chi} = 1, 4\pi$. Upper limits at 90% CL on $\sigma_{\chi-N}$ as a function of m_χ spin-independent (top-right-left) and spin-dependent (top-right-right) interactions, for a coupling strength $\sqrt{g_f g_\chi}$ of unity or the maximum value (4π) that keeps the model within its perturbative regime. The truncation procedure is applied for both cases. Observed lower limits at 95% CL on M_* as a function of M_{med} (bottom), for a Z'-like mediator with vector interactions. For an m_χ of 50 GeV or 400 GeV, results are shown for different values of the mediator total decay width Σ and compared to the EFT observed limit results for a D5 (vector) interaction. M_* vs m_V contours for an overall coupling $\sqrt{g_f g_\chi} = 0.1, 0.2, 0.5, 1, 2, 5, 4\pi$ are also shown. The corresponding limits from the D5 operator are shown as a dashed line. For details see Refs. [6, 8, 9, 20, 21, 24, 26, 29, 31–36]. Plots taken from Ref. [31]

2.2 Mono-photon+ $E_{\mathrm{T}}^{\mathrm{miss}}$

A search using a photon as *tag* object, allow to access three EFT operators (D5, D8 and D9), has been shown in Ref. [31]. Using events with a single highly energetic photon, large $E_{\mathrm{T}}^{\mathrm{miss}}$, no leptons and at most one jet; the main backgrounds in this analysis remain $Z(\nu\nu)+\gamma$, diboson, $W\gamma$ and $Z\gamma$ with lost leptons as well as W and Z production with leptons misidentified as photons. As for the mono-jet search, all measurements are consistent with Standard Model expectations and lower (upper) limits on M_* ($\sigma_{\chi-N}$) are presented both with and without applying the EFT truncation procedure mentioned above, as shown in examples in Fig. 2 (top-left and top-right). In addition limits on M_* as a function of M_{med}, as shown in Fig. 2 (bottom), are derived in the context of a simplified model.

DOI: 10.1051/epjconf/201612004001

2.3 Mono-W/Z+ $E_{\mathrm{T}}^{\mathrm{miss}}$

An analysis using W and Z bosons, respectively their decay products, as *tag* objects gives sensitivity to four EFT operators (C1, D1, D5 and D9) and has been presented in Refs. [37–39], for both hadronic and leptonic decay of the vector bosons. In the analysis aiming at hadronic decays, events are required to contain at least one high-p_{T} *large-radius jet* with reasonably balanced sub-jets, originating from the vector boson; at most one additional *regular* jet; and no leptons and photons. The background yield in the two signal regions, defined by requirements on $E_{\mathrm{T}}^{\mathrm{miss}}$ of 350 GeV and 500 GeV, is dominated by $Z(\nu\nu)$+jets as well as $Z(\ell\ell)$+jets and $W(\ell\nu)$+jets with *lost* leptons. Looking at the leptonic decays, the event selection differs for W or Z bosons. In the first case, events are required to contain exactly one high-p_{T} lepton and a transverse mass of the W boson candidate incompatible with direct production; while in the latter case, events have to contain two leptons giving an invariant mass close to Z peak and no additional lepton or jets. Both cases require large values of $E_{\mathrm{T}}^{\mathrm{miss}}$ and the main background contributions are coming from diboson events in the Z case and in addition $W(\ell\nu)$ and $Z(\ell\ell)$ with *lost* leptons in the W case. All yields are consistent with Standard Model expectations and limits on M_* as a function of m_χ and $\sigma_{\chi-N}$, are presented both for spin-independent and spin-dependent EFT operators, as shown in Fig. 3.

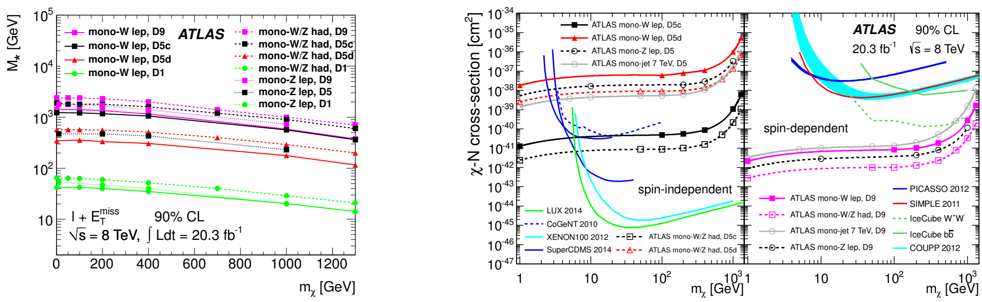

Figure 3. Limits at 90% CL on M_* as a function of m_χ (left), for EFT operators D9, D5 and D1. Observed limits on $\sigma_{\chi-N}$ as a function of m_χ at 90% CL for spin-independent (right-left) and spin-dependent (right-right) operators in the EFT. For details see Refs. [6–9, 29, 30, 32, 34, 35, 37, 38]. Plots taken from Refs. [37–39]

2.4 Heavy-quarks Searches

A search for Dark Matter pair production in association with bottom or top quarks has been presented in Ref. [40]. Aside from being sensitive to three EFT operators (C1, D1 and D9), this analysis also places constraints on the mass of a coloured mediator suitable to explain a possible signal of annihilating Dark Matter, using a simplified model model approach. Several signal regions are defined requiring combinations of increasing jet and b-jet multiplicity, 0 or 1 lepton and values of $E_{\mathrm{T}}^{\mathrm{miss}}$ above 200 GeV to 300 GeV in the events. Applying additional kinematic cuts, the main backgrounds is still coming form $t\bar{t}$-events as well as single-top and W/Z+jets events. All measurements are consistent with Standard Model expectations and lower (upper) limits on $M_*(\sigma_{\chi-N})$ are presented for three EFT operators (C1, D1 and D9), as shown in Fig. 4 for D1operator (top-left and top-right). Due to the proportionality of the scalar operator to the quark mass, limits for D1 are in fact better than those obtained by the above mentioned mono-jet analysis. Constraints on b-flavoured Dark Matter models, using a simplified model, are also presented and shown in Fig. 4 (bottom). For a Dark Matter particle of about 35 GeV, as suggested by an interpretation in Ref. [41] of data recorded by the Fermi–LAT collaboration see Ref. [42], mediator masses between roughly 300 GeV and 500 GeV are excluded at 95% CL.

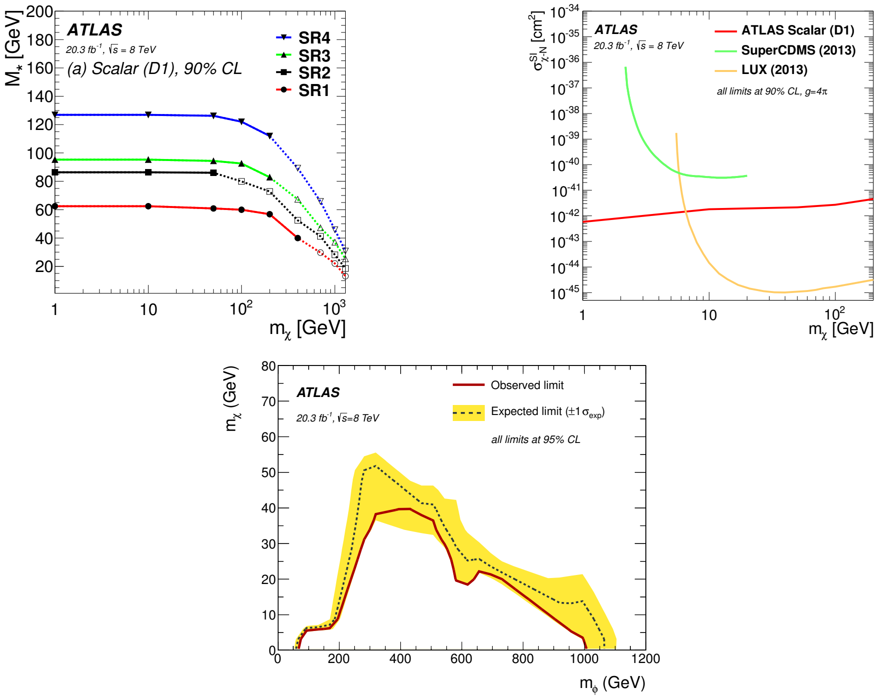

Figure 4. Lower limits on M_* at 90% CL for different signal regions as a function of m_χ (top-left) for the operator D1. Solid lines and markers indicate the validity range of the effective field theory assuming couplings $g_q g_\chi < 4\pi$, the dashed lines and hollow makers represent the full collider constraints. Upper limits at 90% CL on $\sigma_{\chi-N}$ for the scalar operator D1 as a function of m_χ (top-right) compared to other results. The coupling is assumed to be $g_q g_\chi = 4\pi$. Exclusion contour at 95% CL for the b-flavoured Dark Matter model (bottom) from combined results of two signal regions. The expected limit is given by the solid red line. The region beneath the curve indicating the observed limit is excluded. For details see Refs. [6, 7, 40, 43]. Plots taken from Ref. [40]

2.5 Conclusions

The ATLAS Collaboration has performed a broad variety of searches for Dark Matter signatures, using $\sqrt{s} = 8$ TeV Run 1 data and with *tag* objects ranging from single jets, photons, to W/Z bosons and as well as heavy quarks . No signs of Dark Matter have been observed, and stringent limits have set on the different benchmark models, emphasising the complementary nature of collider searches to direct and indirect detection experiments, especially at low Dark Matter masses and for spin-dependent EFT operators.

References

[1] F. Zwicky, Helv. Phys. Acta **6**, 110–127 (1933).

[2] G. Bertone et al. , Phys. Rept. **405**, 279–390 (2005).
[3] G. Jungman et al. , Phys. Rept. **267** , 195–373 (1996).
[4] J. Binney and S. Tremaine, (1993), arXiv:astro-ph/9304010 [astro-ph] .
[5] J. Beringer et al. (Particle Data Group), Phys. Rev. **D86**, p. 010001Jul (2012).
[6] D. S. Akerib et al. (LUX Collaboration), Phys. Rev. Lett. **112** , p. 091303 (2014).
[7] R. Agnese et al. (SuperCDMS Collaboration), Phys. Rev. Lett. **112** , p. 041302 (2014).
[8] E. Behnke et al. (COUPP Collaboration), Phys. Rev. D 86, p. 052001Sep (2012).
[9] S. Archambault et al. (PICASSO Collaboration), Phys. Lett. **B711**, 153?161 (2012).
[10] M. Beltran et al. , JHEP **09** , p. 037 (2010).
[11] P. J. Fox et al. , Phys. Rev. **D85**, p. 056011 (2012).
[12] J. Goodman et al. , Phys. Rev. **D82**, p. 116010 (2010).
[13] ATLAS Collaboration, JINST **3**, p. S08003 (2008).
[14] ATLAS Collaboration, Eur. Phys. J. **C75** , p. 299 (2015).
[15] CMS Collaboration, Eur. Phys. J. **C75**, p. 235 (2015).
[16] P. A. R. Ade et al. (Planck Collaboration), Astron. Astrophys. **571**, p. A16 (2014),
[17] G. Hinshaw et al. , ApJS **208**, p. 19 (2013)
[18] M. Ackermann et al. (Fermi-LAT Collaboration), Phys. Rev. **D89**, p. 042001 (2014)
[19] A. Abramowski et al. (H.E.S.S. Collaboration), Phys. Rev. Lett. **106**, p. 161301 Apr(2011).
[20] G. Angloher et al. , Eur. Phys. J. **C72**, p. 1971 (2012)
[21] R. Agnese et al. (CDMS Collaboration), Phys. Rev. Lett.**111**, p. 251301 (2013).
[22] R. Agnese et al. (SuperCDMS Collaboration), Phys. Rev. Lett. **112**, p. 241302 (2014).
[23] C. E. Aalseth et al., (2014), arXiv:1401.6234 [astro-ph.CO]
[24] R. Bernabei et al. (DAMA Collaboration), Eur. Phys. J. **C56**, 333–355 (2008).
[25] E. Aprile et al. (XENON100 Collaboration), Phys. Rev. Lett.**111** , p. 021301 (2013).
[26] S. Desai et al. (Super-Kamiokande Collaboration), Phys. Rev. **D70**, p. 083523 (2004).
[27] R. Abbasi et al. (IceCube Collaboration), Phys. Rev. Lett. **102** , p. 201302May (2009).
[28] E. Behnke et al. (COUPP Collaboration), Phys. Rev. Lett. **106**, p. 021303Jan (2011).
[29] M. Felizardo et al. (The SIMPLE Collaboration), Phys. Rev. Lett. **108**, p. 201302May (2012) .
[30] ATLAS Collaboration, ATL-PHYS-PUB-2014-007 (2014). https://cds.cern.ch/record/1708859 .
[31] ATLAS Collaboration, Phys. Rev. **D91**, p. 012008 (2015).
[32] E. Aprile et al. (XENON100 Collaboration), Phys. Rev. Lett. **109**, p. 181301Nov (2012).
[33] Z. Ahmed et al. (CDMS Collaboration), Phys. Rev. Lett. **106**, p. 131302Mar (2011).
[34] C. E. Aalseth et al. (CoGeNT Collaboration), Phys. Rev. Lett. **106**, p. 131301Mar (2011).
[35] M. G. Aartsen et al. (IceCube Collaboration), Phys. Rev. Lett. **110**, p. 131302Mar (2013).
[36] A. Abramowski et al. (HESS Collaboration), Phys. Rev. Lett. **110**, p. 041301 (2013).
[37] ATLAS Collaboration, Phys. Rev. Lett. **112**, p. 041802 (2014).
[38] ATLAS Collaboration, JHEP **09**, p. 037 (2014).
[39] ATLAS Collaboration, Phys. Rev. **D90**, p. 012004 (2014).
[40] ATLAS Collaboration, Eur. Phys. J. **C75** , p. 92 (2015).
[41] T. Daylan et al. , (2014), arXiv:1402.6703 [astro-ph.HE] .
[42] W. B. Atwood et al. , The Astrophysical Journal **697** , p. 1071 (2009).
[43] R. Gaitskell et al. , http://dmtools.brown.edu/.